PROGRESS IN PHOTOVOLTAICS: RESEARCH AND APPLICATIONS
Prog. Photovolt: Res. Appl. 2008; **16**:307–315
Published online 21 February 2008 in Wiley InterScience (www.interscience.wiley.com) DOI: 10.1002/pip.813

Research

Assessing the Outdoor Operating Temperature of Photovoltaic Modules

David Faiman*,†
Department of Solar Energy & Environmental Physics, Jacob Blaustein Institutes for Desert Research, Ben-Gurion University of the Negev, Sede Boqer Campus 84990, Israel

By a careful study of data collected from seven varieties of photovoltaic (PV) module it is demonstrated that a simple modified form of the Hottel–Whillier–Bliss (HWB) equation, familiar from the analysis of flat-plate solar–thermal collectors, can be employed to predict module temperatures within an accuracy comparable to the cell-to-cell temperature differences typically encountered within a module. Furthermore, for modules within the range of construction parameters employed in this study, the actual values of the two modified HWB constants do not appear to depend upon module type. The implication of these results for the accuracy of outdoor module characterization is discussed. Copyright © 2008 John Wiley & Sons, Ltd.

KEY WORDS: PV module temperature; Hottel–Whillier–Bliss

Received 16 August 2007; Revised 5 November 2007

INTRODUCTION

The instantaneous temperature of a photovoltaic (PV) module depends upon the incoming solar irradiance, the module's electrical, optical, and thermal properties, and its heat exchange with the surroundings. The earliest attempt to employ basic heat transfer techniques, long-familiar from the modeling of solar–thermal collectors,[1] to a PV system appears to have been by Florschuetz,[2] who modeled a combined PV and solar hot water system. However, because of the large thermal mass of the water the actual temperature of any part of the system, at any given instant, depends upon the solar irradiance received at earlier times. For this reason the mathematical formalism employed by Florschuetz was possibly more cumbrous than would be needed for modeling a simple PV panel with no water ducts. Fuentes[3] modeled arrays of PV modules, *per se*, but because they formed part of a more massive roof structure, his formalism was almost as complicated as that needed for a water-cooled module. More recently, Notton *et al*.[4] employed basic heat transfer principles to model a PV module that was glazed on both its front and rear surfaces. For such a massive structure it is to be expected that the actual cell temperature may be higher at times than the corresponding temperature of the rear glass surface where one would normally try to measure the module temperature, and such was indeed found to be the case by these authors. Accordingly, once again, a full-blown heat transfer approach that considered energy flows among the various components of the module and between its cover glasses and the surroundings was found necessary in order to be able to understand their experimental data.

* Correspondence to: David Faiman, Department of Solar Energy & Environmental Physics, Jacob Blaustein Institutes for Desert Research, Ben-Gurion University of the Negev, Sede Boqer Campus 84990, Israel.
†E-mail: faiman@bgu.ac.il

Our approach differs from that of previous authors in that we assume the thermal mass of a conventional (i.e., glass front, plastic back) PV panel to have a negligible effect on its heat exchange with the surroundings. This enables us to start from a simplified heat transfer formalism that was originally developed for flat-plate solar-thermal collectors under conditions of steady state, namely the so-called Hottel–Whillier–Bliss equation:[5,6]

$$\eta = \eta_o - (U/H)(T - T_{amb}) \quad (1)$$

This equation states that the efficiency η of a solar–thermal collector under steady state conditions is the difference of two parts: a temperature-independent optical part η_o, and a thermal part that increases from zero with increasing collector temperature above ambient T_{amb}. The heat transfer coefficient U, which lumps together the effects of conduction, convection and radiation exchange, is itself temperature-dependent, but can be linearized over any sufficiently narrow range of temperatures that may be of interest. H is the total irradiance incident on the collector surface at that instant.

The utility of our proposed method is that: (a) it uses a simple, heuristic, algebraic equation to predict module temperature, given the ambient temperature, the incident irradiance, and the wind speed; (b) it requires only two numerical constants, the values of which may be derived from a simple experiment; (c) the RMS accuracy of the predictions, as we shall demonstrate, is comparable to the cell-to-cell temperature differences observed within any given PV module.

EXPERIMENTAL SETUP

Figure 1 shows an equator-facing, tilt = latitude stand, of a type that is commonly employed for achieving maximum year-round energy collection for static PV modules. The stand contains PV modules of (mono- and poly-) crystalline silicon cells, with power ratings in the 140–220 Wp range, made by seven different manufacturers. Depending upon the specific module, the cell colors are various shades of blue. All modules have glass covers and Tedlar™ backs. The stand is located at Sede Boqer in the Negev Desert (Lat. 30·9°N, Long. = 34·8°E, Elevation = 470 m).

Each module is connected to a resistive load that operates it reasonably close to its maximum power point during that part of the day when most of the energy is normally produced. The stand also contains a thermopile pyranometer (type Eppley PSP) for monitoring plane of array (POA) irradiance. To the rear of each module two thermocouples (TCs) are attached: one behind a central cell and the other behind a cell in the lower corner of the module. Each TC is attached using a small bead of quick-drying epoxy putty. The bead is applied in a manner that presses the TC junction to the Tedlar™ cell backing, while at the same time providing some shielding of the TC from the immediate effects of fluctuating wind speeds. The physical size of the bead (approximately 5 mm in diameter) is deemed sufficiently small not to interfere with the natural temperature of the cell to which it is attached.

Figure 1. Test stand of PV modules as viewed from the south. The small PV module (upper left, next to the pyranometer) provides a trickle charge for the data logger located behind the array. The data logger records seven pairs of module temperatures and POA irradiance as 5-min averages

A Campbell 21X data logger samples all 14 TCs and the pyranometer every 10 s, and stores 5-min averages.

In addition to these data, wind speed at a height of 3·5 m above ground, and ambient temperature are monitored (on the same time scale) at a meteorological station located approximately 100 m south of the PV array. Since the prevailing winds are from the NW, and clear desert terrain separates the PV array from the meteorological station, we consider data from the latter to be reasonably representative of results that would have been obtained had the ambient temperature and wind measurements been taken closer to the PV modules.

DOI: 10.1002/pip

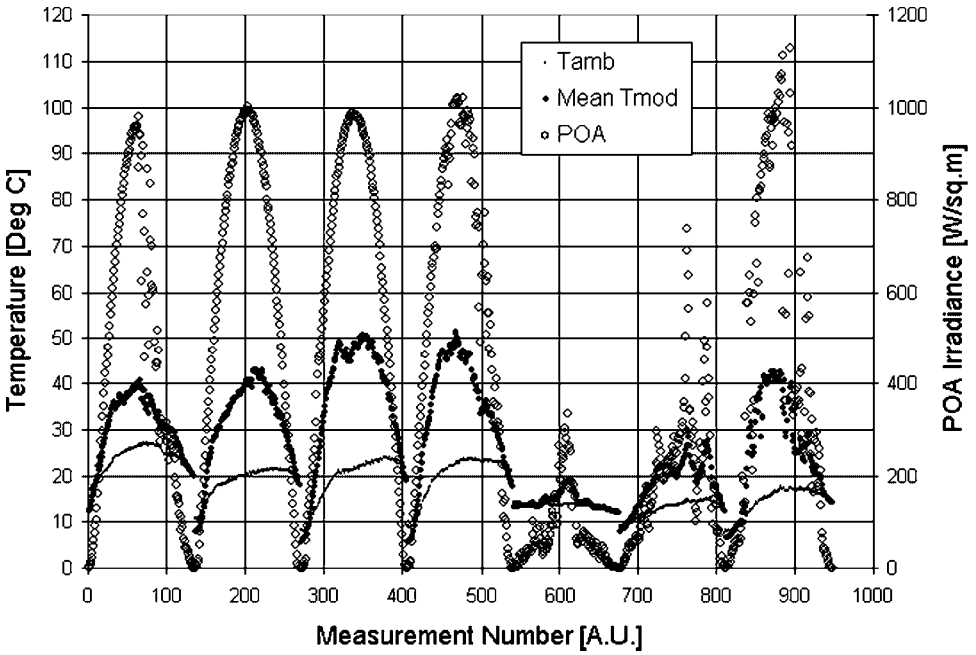

Figure 2. Daytime data for the week 1–7 November 2006. Open circles, triangles and solid circles represent, respectively, POA irradiance, mean module temperature, and ambient temperature

TRENDS AMONG THE DATA

Figure 2 displays POA irradiance, ambient temperature, and the average output of the 14 TCs for daylight hours (defined as periods for which the POA pyranometer gave a non-negative reading) during the first week of November 2006. This specific week was chosen because it contains a representative sampling of most of the weather conditions that may be expected to occur in a desert setting. Specifically, a dust storm during the afternoon of November 1; followed by two basically cloudless days; a cloudy but bright day; a rainy day (all day); and two final days with successively less cloudiness.

Figure 3 shows the corresponding data during the nighttime periods (defined as all data not included in Figure 2) for the same week. Also shown in Figure 3 is the nighttime wet-bulb temperature.

Cell-to-cell temperature differences within a module

The first question of interest is: *Is there any systematic difference in temperature between a center cell and a corner cell?*

Table I displays the mean temperature difference and root-mean-square (RMS) difference between the monitored center and corner cell for each of the seven modules, calculated separately over the 942 5-min daytime data and the 1157 nighttime data, during this first week of November 2006.

The first important point to notice is that the nighttime data display an RMS difference of $0{\cdot}26 \pm 0{\cdot}04$ K between the center cell and the corner cell in any given module. Note, moreover, that the difference is not systematic: there being a positive difference for five modules and a negative difference for two. Had all the differences been consistently negative or positive, we might have inferred that perhaps the corner cells are more subject to warming by the ambient air than are the center cells, or *vice versa* (all cells being evidently subject to nocturnal radiation cooling, as seen in Figure 2). But this is not the case. Now a daytime difference of whatever magnitude and sign could be understandable in terms of differing electrical properties among the cells in a given module, but at night there should be no temperature difference from cell-to-cell. We therefore infer that the apparent RMS nighttime difference of $\pm 0{\cdot}26$ K represents the level of accuracy below which we cannot measure temperatures with TCs attached in the manner indicated.

Turning now to the daytime temperature differences in Table I, we observe a clear tendency for the center

DOI: 10.1002/pip

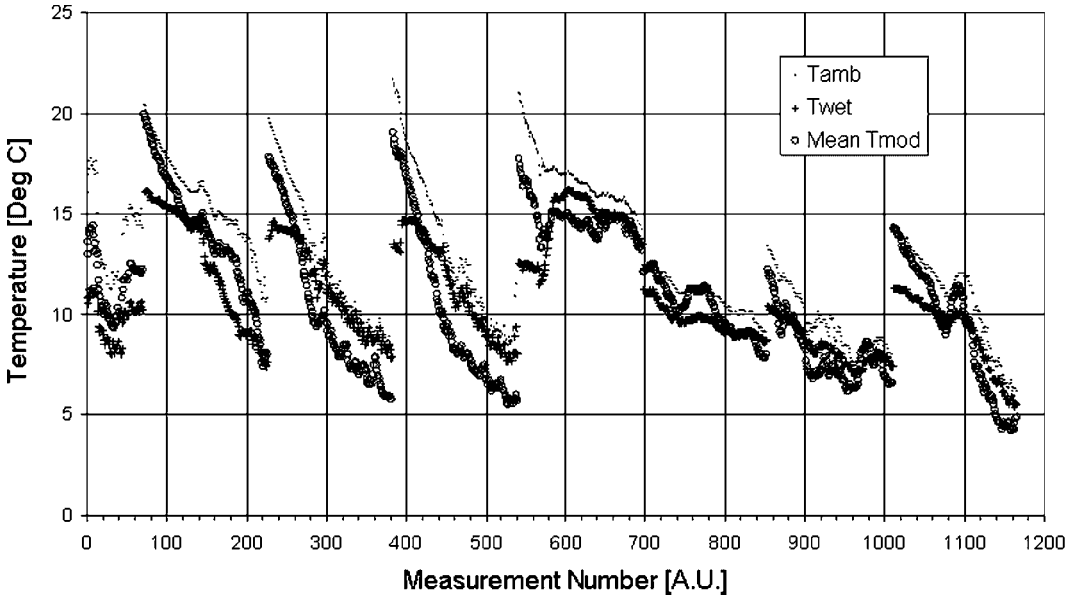

Figure 3. Nighttime data for the week 1–7 November 2006. Solid circles, open circles, and triangles indicate, respectively, ambient temperature, wet-bulb temperature, and mean module temperature

cell to be warmer than a corner cell, the RMS difference being 2·06 K. The only apparent exception is module no.1 with a small negative value for this temperature difference. However, because its magnitude is far smaller than the 0·26 K accuracy discussed in the previous paragraph, it is of no physical significance. Six of the modules indicate a clear positive temperature difference for the center cell over the corresponding corner cell. The probability of this being a random result is 3% if we do not expect a positive difference, and 1·6% if we do expect this difference to be positive. Since the corner cells are less heated by surrounding hot cells than are the central cells, there are indeed physical grounds for expecting a temperature difference with the observed sign. However, be that as it may, our experimental measurements present clear indication that the central cells are typically 2 K warmer than the corner cells. Therefore, in any attempt to predict module temperatures, it must be kept in mind that within any given module we must expect to have cell-to-cell temperature differences of approximately 2 K.

Module-to-module temperature differences

The second question of interest is: *Are there any significant differences in temperature among the various modules?* In order to study this question we

Table I. Average differences and RMS differences between the center-cell and corner-cell temperatures for the seven test modules, separated according to daytime and nighttime, during the first week of November 2006

Module no.	$<T_{center} - T_{corner}>$ (K)		RMS temp. difference (K)	
	Day	Night	Day	Night
1	−0·08	+0·20	1·99	0·26
2	+1·37	+0·08	2·26	0·25
3	+0·31	+0·18	1·84	0·26
4	+0·99	+0·29	2·01	0·36
5	+1·54	−0·12	2·25	0·25
6	+1·12	−0·02	2·09	0·23
7	+1·37	+0·00	1·97	0·21
Average	+0·94	+0·09	2·06	0·26

DOI: 10.1002/pip

Table II. Average difference and RMS difference of the mean daytime module temperature for each of the seven test modules, from the average over all modules, during the first week of November 2006

Module no.	$<T_{mod} - T_{avg}>$ (K)	RMS temp. difference (K)
1	−0·19	0·71
2	−0·37	0·75
3	−0·36	0·55
4	+0·21	0·55
5	−0·16	0·62
6	+0·19	0·70
7	+0·68	1·07
Average	0	0·71

first take the average of the center and corner temperature for each module as being representative of the mean module temperature T_{mod} during daytime. We then compare these individual mean temperatures with the average T_{avg} taken over all seven modules. The results are shown in Table II.

Table II indicates that the individual modules exhibit an RMS spread of 0·71 K relative to the average taken over all modules. Since all modules are subject to identical ambient conditions we may infer that even though they are the products of different manufacturers, some containing mc-Si and others pc-Si cells, the cell temperatures are not significantly different from module to module, for the sample of modules in this study. That is to say, the module-to-module differences are less than the cell-to-cell differences within a module. One also notices from Table II that the temperature difference between the two extreme modules (nos. 2 and 7) is comfortably less than the 2 K cell-to-cell temperature difference we observed above that exists within any given module. For this reason, the bulk of our comparisons between theory and experimental data will address data averaged over all seven modules. We shall, however, return to the question of module-to-module differences later.

THEORETICAL EXPECTATIONS

By multiplying Equation (1) by H, we obtain an expression for the useful thermal power ηH that can be extracted from a flat-plate collector under steady-state conditions:

$$\eta H = \eta_o H - U(T - T_{amb}) \quad (2)$$

If the collector could produce electrical power in addition to thermal power, then the amount of thermal power that could be extracted would be less than that given in Equation (2), namely

$$\eta H = \eta_o H - U(T - T_{amb}) - \eta_e H \quad (3)$$

where η_e is the electrical efficiency of the collector at temperature T.

Under conditions of thermal stagnation—that is, when the useful *thermal* power drops to zero, the thermal efficiency η becomes zero, and the collector reaches its maximum or "stagnation" temperature:

$$T_{stag} = T_{amb} + H(\eta_o - \eta_e)/U \quad (4)$$

Now, because a PV module has very little thermal mass compared to a water-heating collector, Equation (4) should yield a reasonable representation of the module temperature T_{mod}, even under conditions of varying irradiance and wind speed v. To allow for the effect of wind, it should be sufficient to parameterize U as $U_0 + U_1 \times v$, where U_0 and U_1 are constants.

We therefore expect that the temperature of a PV module should be given to a good approximation by the expression

$$T_{mod} = T_{mod} + H/(U_0' + U_1' \times v) \quad (5)$$

where

$$U_0' = U_0/(\eta_o - \eta_e) \text{ and } U_1' = U_1'/(\eta_o - \eta_e)$$

Note, however, that the optical efficiency η_o of a glass-covered water-heating collector is typically a constant in the range 0·8–0·9, whereas the electrical efficiency η_e of a PV module would typically be a number that hovers around 0·1 for all normal operating temperatures. Therefore, their difference should take a value that fluctuates relatively slightly about a value close to 0·7. From Equation (5) we should accordingly expect that by plotting $H/(T_{mod} - T_{amb})$ against v, a straight line should result, with relatively small scatter. Moreover, the slope U_1' and intercept U_0' of this line should each be approximately constant.

THEORY VERSUS EXPERIMENT

Figure 4 shows a plot of $H/(T_{mod} - T_{amb})$ against v. For T_{mod} we have used the average temperature registered by all 14 TCs. Furthermore, we have cut the data so as to include only those 5-min averages that fall between

DOI: 10.1002/pip

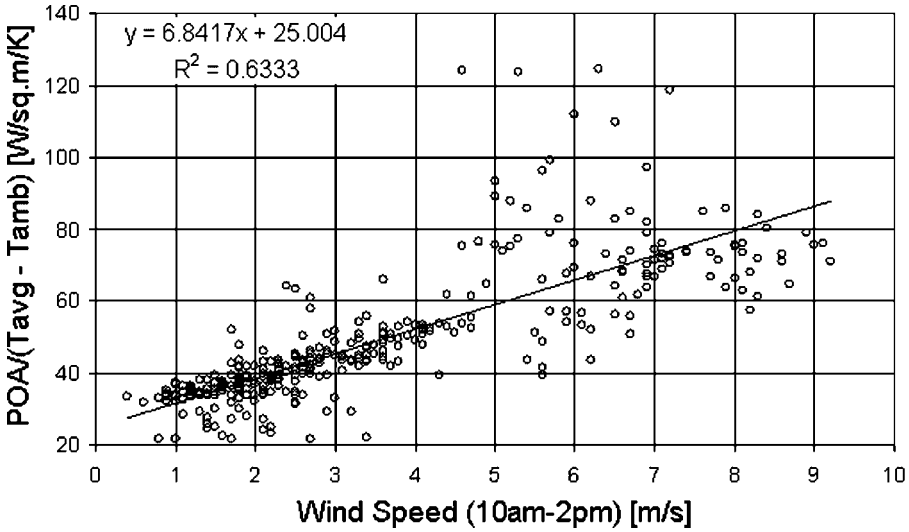

Figure 4. Plot of $H/(T_{\mathrm{mod}} - T_{\mathrm{amb}})$ versus wind speed v, and associated least squares linear fit to the data, for all 5-min data points in the daily time interval 10 am to 2 pm

the hours of 10 am and 2 pm. The reason for such data selection is to reduce the amount of noise caused by dividing small numbers by small numbers, as can happen early or late in the day. The data in Figure 4 show the expected trend very clearly, the least-squares fit having an intercept value $U_0' = 25{\cdot}0\,\mathrm{W\,m^{-2}\,K^{-1}}$, and a slope value $U_1' = 6{\cdot}84\,\mathrm{W\,m^{-3}\,s\,K^{-1}}$, with $R^2 = 0{\cdot}63$.

These least-squares fit values of U_0' and U_1' may now be used in conjunction with Equation (5) to predict module temperatures if we know the corresponding ambient temperature, wind speed, and POA irradiance. In particular, taking *all* 942 of the (daytime) ambient temperature, wind speed, and irradiance data recorded during this one-week time period, we have predicted the corresponding module temperatures. The results are shown as a scatter plot in Figure 5, which compares the predictions with their corresponding measured values. In Figure 5 we have distinguished between the 343 data points from 10 am to 2 pm (solid circles) that were employed for deriving the parameters U_0' and U_1', and the 599 sunrise-to-10 am and 2 pm-to-sunset points (open circles) that are true predictions of the theory.

In spite of the seemingly large scatter in Figure 4, the resulting temperature predictions (for all 942 5-min averages) have an RMS error of only 1·86 K.

From Figure 5 it is clear that Equation (5) represents the overall trend of the data extremely well, over the entire module temperature range of 5–50°C observed during the week in question. Moreover, quantitatively, the RMS error of $\pm 1{\cdot}86$ K between theory and experiment is again comparable to the observed cell-to-cell temperature within any given module. It is true that the early morning temperatures are predicted to be slightly higher than those observed. This is due to the fact that the solar radiation at this hour was not yet strong enough to have warmed the modules completely above their nighttime sub-ambient temperatures. Furthermore, there are also a number of isolated scattered points that are several degrees outside the RMS range. These were probably caused by gusting winds producing non-symmetric module temperature fluctuations during some of the 5-min averages that constitute our experimental data set. But on the whole, the agreement between theory and experiment is seen to be as good as one can reasonably expect. This can be seen, perhaps more compellingly, from Figure 6 which re-plots the data of Figure 5 in their true time sequence.

MODULE TO MODULE DIFFERENCES

Having thus far averaged all temperature data over the seven different modules, it is now interesting to see the extent to which the heat loss coefficients we obtained by using data averaged over all the modules may differ from what we would have obtained had we analyzed each of the modules individually. We have accordingly repeated the analysis discussed above, for each module individually. The results are shown in Table III.

DOI: 10.1002/pip

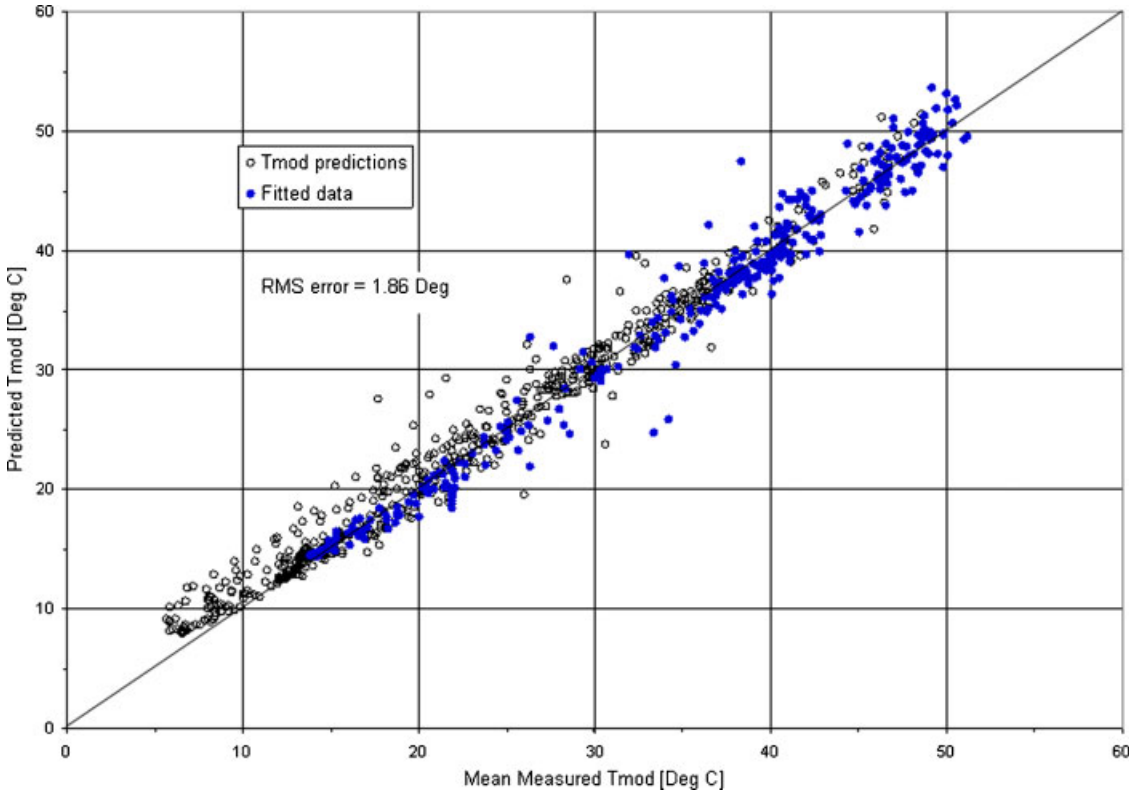

Figure 5. Comparison of predicted mean module temperature with measured mean module temperature for *all* 942 daytime data points measured during the first week of November 2006. The 599 open circles are true predictions of the theory. The 343 solid circles are data used for fitting purposes

Referring to Table III, the average of the seven U_0' values is $24{\cdot}9 \pm 1{\cdot}0\,\mathrm{W\,m^{-2}\,K^{-1}}$. Similarly, the average of the seven U_1' values is $7{\cdot}00 \pm 0{\cdot}55\,\mathrm{W\,m^{-3}\,K^{-1}}$. We thus see that, for this set of modules, the standard deviation in U_0' is 4% of the mean value, and the standard deviation in U_1' is 8% of its mean value. The values of both parameters we derived from the combined fit fall comfortably within the 1 σ spread.

It is worth pointing out that knowledge of U_0' and U_1' enables one to employ Equation (5) in order to calculate the so-called nominal operating cell temperature (NOCT) of a module.[7] This is defined as the module temperature at $800\,\mathrm{W\,m^{-1}}$ irradiance, 20°C ambient temperature, and $1\,\mathrm{m\,s^{-1}}$ wind speed. Perusal of Table III enables one to see that for all of the modules considered here, NOCT is close to 45°C.

CONCLUSIONS

By examining 1 week of 5-min average data, collected simultaneously from seven different brands of PV module, we conclude that owing to cell-to-cell temperature differences within a module, module temperatures cannot be defined to an RMS precision of better than about ± 2 K. Furthermore we find that within this degree of precision, a modified HWB equation, Equation (5), can be used to predict module temperatures, using as input, ambient temperature, wind speed, plane-of-array irradiance, and a pair of heat loss coefficients U_0' and U_1' that can be determined by a simple experimental procedure which we have illustrated. Furthermore, since the power ratings of c-Si cell modules typically have temperature coefficients in the neighborhood of $0{\cdot}5\%\,\mathrm{K^{-1}}$, an uncertainty of 2 K in module temperature represents an error of only 1% in power.

As a noteworthy corollary, the experimental considerations discussed above provide quantitative indication of the level of precision that may meaningfully be expected of *any* theoretical model that seeks to predict module temperatures from environmental measurements. We may accordingly conclude that the RMS spread of $\pm 1{\cdot}86$ K apparent in the

DOI: 10.1002/pip

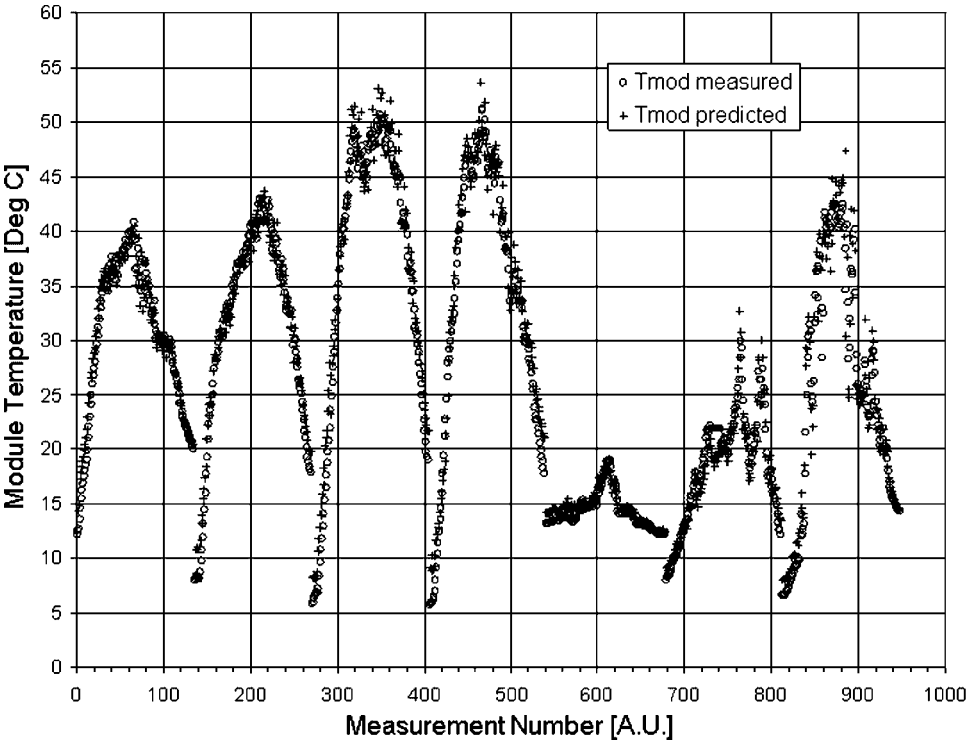

Figure 6. True-time comparison of predicted module temperature (bullets) with measured mean module temperature (open circles) for all 942 daytime data points measured during the first week of November 2006

predictions of a modified HWB equation are of adequate accuracy for this purpose, and that should a theoretically superior equation be derivable, it would have no practical value.

Although we found an approximately universal pair of heat-loss coefficients for all seven module brands under study, we caution that the specific values we obtained for these coefficients may well depend, to a certain extent, upon:

(a) The local environment. Our modules were mounted on an open rack, the rear surfaces of the modules being subjected to convective cooling by the prevailing winds, and to radiation exchange with desert sand. The situation for roof-integrated modules, as indicated by Fuentes[3] is evidently more complicated.

(b) The specific cell material from which the modules are fabricated. We have studied only those with mc-Si and pc-Si cells. Different numerical coefficients may arise from cells fabricated from a-Si or non-silicon materials.

(c) Module encapsulation. Our modules had front glass covers and Tedlar™ backs. Modules with

Table III. Heat loss coefficients for the individual modules, and RMS errors relative to their respective data sets

Module type	U_0' ($W\,m^{-2}\,K^{-1}$)	U_1' ($W\,m^{-3}\,s\,K^{-1}$)	RMS error (°C)
Solarwatt MHH plus 170	24·1	7·12	2·13
Solar-Fabrik SF 150/2-142	24·0	7·68	2·12
Solar World SW200 poly	25·7	7·25	1·88
RWE Schott Solar ASE-165-GT-FT/MC	23·5	7·66	1·96
Shell Solar Power Max Plus 165-C	25·7	6·68	1·93
Scheuten Multisol 180 P6	26·4	6·25	1·85
Solon P220/6+	24·9	6·33	1·99
Combined Fit	25·0	6·84	1·86

DOI: 10.1002/pip

non-glass front surfaces may yield numerically different values for the parameters U_0' and U_1'. Moreover, modules with glass rear surfaces, as indicated by Notton *et al*.,[4] may well require a more complicated theoretical treatment. At the very least, should our present approach turn out to provide a satisfactory fit to data from such modules, there would still remain the problem of determining the effective cell temperature from the measured rear-surface temperature.

However, the main message of this work is that, at least for the widely used kind of modules we have studied, Equation (5) can be used for the prediction of module temperatures to a degree of precision that is as high as can be meaningful under outdoor conditions. All that is needed are a few days of *in situ* module temperature data in order to derive appropriate values of U_0' and U_1' for the module type and location in question. The results should then enable the power of a module to be determinable to a precision of the order of $\pm 1\%$ by outdoor measurement under suitably stable weather conditions.[8]

Acknowledgements

This sub-project of a German research project is jointly funded by: the German Federal Ministry for the Environment (Contract No. 0329978); the manufacturers; Scheuten Solar, Schott Solar, Solarfabrik, Solarwatt, Solarworld, Solon; Fraunhofer ISE, Freiburg, and TÜV Rheinland, Cologne. The author wishes to thank Dr. Michael Koehler and Dr. Werner Hermann for stimulating discussions and for handling logistics at the European end. He also wishes to express his indebtedness for technical assistance to Dov Bukobza, Shlomo Kabalo and Vladimir Melnichak.

REFERENCES

1. Kreith F, Kreider JF. *Solar Energy Engineering*. McGraw-Hill: New York, 1978.
2. Florschuetz LW. Extension of the Hottel–Whillier model to the analysis of combined photovoltaic/thermal flat plate collectors. *Solar Energy* 1979; **22**: 361–366.
3. Fuentes MK. Thermal model of residential photovoltaic arrays. *Proceedings of 17th IEEE PV Specialists Conference,* 1984; 1341–1346.
4. Notton G, Cristofari C, Mattei M, Poggi P. Modelling of a double-glass photovoltaic module using finite differences. *Applied Thermal Engineering* 2005; **25**: 2854–2877.
5. Hottel HC, Whillier A. Evaluation of flat plate collector performance. *Transactions of the Conference on the Use of Solar Energy, Vol. 2, Part 1, University of Arizona Press,* 1958; p. 74.
6. Bliss RW. The derivations of several 'plate efficiency factors' useful in the design of flat-plate solar-heat collectors. *Solar Energy* 1959; **3**: p. 55.
7. Stultz JW. Thermal and other tests of photovoltaic modules performed in natural sunlight. *Journal of Energy* 1979; **3**: 363–372.
8. Berman D, Faiman D, Farhi B. Sinusoidal spectral correction for high precision outdoor module characterization. *Solar Energy Materials and Solar Cells* 1999; **58**: 253–264.

DOI: 10.1002/pip